Marine and Petroleum Geology 165 (2024) 106892

Contents lists available at ScienceDirect

Marine and Petroleum Geology

journal homepage: www.elsevier.com/locate/marpetgeo

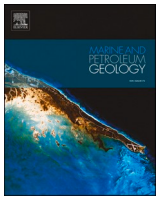

Time-calibration of carbonate diagenesis and regional tectonism in the Norwegian Barents Sea

Malcolm S.W. Hodgskiss [a,*], Nick M.W. Roberts [b], Michał Matysik [c], Päärn Paiste [d], Niels Rameil [e], Erik Hammer [e], Jon Halvard Pedersen [e], Harald Brunstad [e], Aivo Lepland [a]

[a] Geological Survey of Norway, Trondheim 7040, Norway
[b] Geochronology and Tracers Facility, British Geological Survey, Nottingham, NG12 5GG, United Kingdom
[c] Institute of Geological Sciences, Jagiellonian University, Gronostajowa 3a, 30-387, Kraków, Poland
[d] Department of Geology, University of Tartu, Tartu 50411, Estonia
[e] Aker BP ASA, Lysaker 1366, Norway

A B S T R A C T

Diagenesis plays a crucial role in carbonate reservoir properties, for example through the dissolution or precipitation of carbonate minerals, with burial history and fluid migration thought to play an important role in the timing of these events. To better understand these relationships and the local manifestation of regional events, we study carbonate sedimentary rocks and associated diagenetic cements from the Loppa High and Finnmark Platform using in-situ U–Pb carbonate geochronology and C–O stable isotope ratios, combined with burial history modelling. The results indicate a complex history of diagenesis: analyzed dolomicrite samples from the Loppa High typically yield ages that are older than their biostratigraphic age, in contrast to dolomicrite samples from the Finnmark Platform that yielded younger ages; this regional offset may be reflective of different styles of early diagenesis, as well as heterogeneous and re-deposited origin of some studied materials. While many diagenetic calcite cements coincide with modelled burial or uplift events, other events have no cements associated with them, although the possibility that some diagenetic carbonate phases were unsampled cannot be ruled out. Some calcite cements are not associated with burial events at all and may instead be related to hydrocarbon 'charging', supported by strongly negative $\delta^{13}C$ values recorded in these cements. Broadly, these results highlight the value of integrating petrographic observations, burial history modelling, carbonate U–Pb geochronology, and C–O isotope ratios, as well as the complexity of untangling diagenetic histories.

1. Introduction

Diagenesis plays a key role in controlling the properties of carbonate reservoirs, and can both positively and negatively impact pore space, connectivity, and other variables through the dissolution or precipitation of carbonate minerals (e.g., Lucia et al., 2003; Hollis, 2011). Developing a robust understanding of diagenetic processes and events, both in terms of their driving mechanisms and timing, is therefore crucial for characterizing carbonate petroleum reservoirs. Thankfully, carbonate minerals record a wealth of geochemical information on their precipitation conditions through a wide range of isotopic and elemental ratios, such as $\delta^{13}C$ and $\delta^{18}O$ to assess fluid sources and precipitation conditions and U–Pb isotope ratios to determine timing of precipitation (e.g., Lan et al., 2022, 2023).

Recent studies of the timing of carbonate diagenesis have indicated that while regional-scale events such as magmatism or burial/uplift play an important role, there is significant variability at the local scale, with, for example, the ages of diagenetic cements varying between drill cores from the same structural element (e.g., Hodgskiss et al., 2024). In this study, we combine the aforementioned geochemical techniques with observations of mineral paragenesis and burial history modelling to reconstruct diagenetic events. We examine Carboniferous to Triassic strata from the Loppa High and Finnmark Platform in the Norwegian Barents Sea (Fig. 1), both of which have undergone distinct burial histories and carbonate mineral precipitation and reprecipitation events spanning from eogenetic to telogenetic (very early to very late) to explore the relationship between burial history and diagenesis at the regional and local level.

2. Geological setting and lithological units

The Norwegian sector of the Barents Sea is divided into more than 30 distinct structural elements representing various depositional basins, platforms, and highs, and it records a complex history of compressional, extensional, and transverse tectonism that spans hundreds of millions of years (Gabrielsen et al., 1990). Sedimentary rocks composing the

* Corresponding author.
E-mail address: mhodgskiss@gmail.com (M.S.W. Hodgskiss).

https://doi.org/10.1016/j.marpetgeo.2024.106892
Received 11 December 2023; Received in revised form 17 April 2024; Accepted 3 May 2024
Available online 4 May 2024

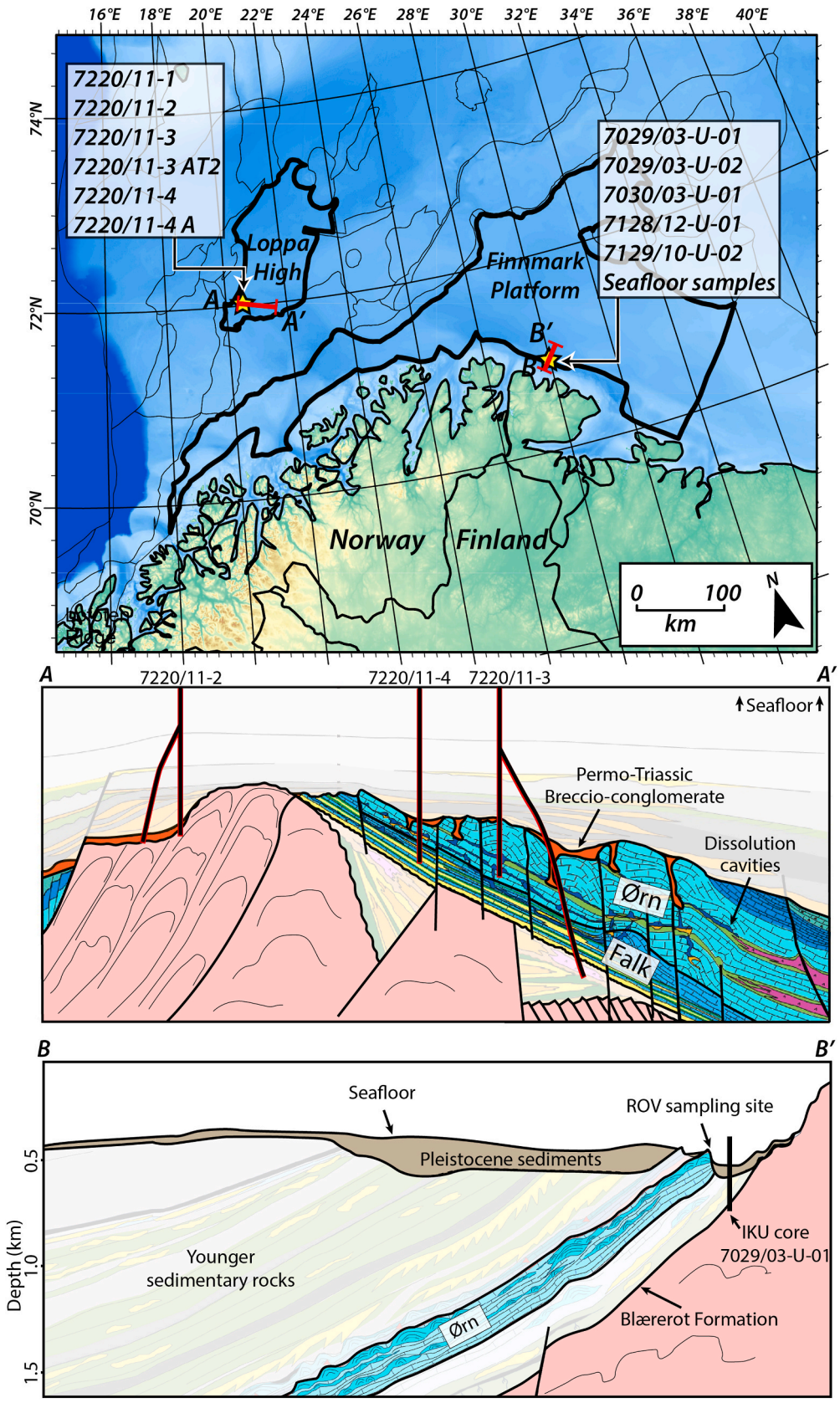

Fig. 1. Map of structural elements of the Barents Sea, with the Loppa High and Finnmark Platforms emphasized with bolded lines. The location of studied drill cores and seafloor samples are marked with stars. Loppa High cross section is schematic; in this region the Falk, Ørn, and P-T Breccio-conglomerate reach thicknesses up to 250, 115, and 90 m, respectively, with significantly variations occurring due to truncation, wedging, and paleotopography. The Blærerot Formation, which was studied on the Finnmark Platform, is too thin to be shown.

bedrock geology of the Barents Shelf extend over approximately 1.4 million km^2 and span from the Ordovician to Cenozoic, making the area one of the largest and longest-lived epicontinental basins in the world (Henriksen et al., 2011; Lammers et al., 1995; Midtkandal et al., 2019). A brief tectonostratigraphic overview of relevant structural elements of the Norwegian sector is presented here, as well as detailed descriptions for the studied stratigraphic units (Blærerot Formation, Ørn Formation, and Permo-Triassic breccio-conglomerate).

2.1. Loppa High

The Loppa High structural element contains strata ranging from the Devonian to Paleocene (Brunstad and Rønnevik, 2024). Strike-slip faulting during the Devonian resulted in the formation of narrow basins (Rønnevik and Jacobsen, 1984), and Carboniferous rifting and wrenching formed half-grabens (Stemmerik et al., 1991; Stemmerik and Worsley, 1989). Rifting during the Late Permian to Mid-Triassic resulted in subaerial exposure of the crest of the Paleo Loppa High (or Selis Ridge), and subsequent erosion of as much as 500 m of stratigraphy, ultimately redeposited in flanking basins (Sayago et al., 2012; Clark et al., 2014). The Late Triassic saw subsidence of the Loppa High and the deposition of thick clastic sediment packages (Glørstad-Clark et al., 2010). The region experienced overall subsidence during the Late Jurassic and through the Cretaceous-Paleogene transition, albeit interrupted by several phases of extensional and transform tectonism resulting in several intervals of uplift and erosion (Glørstad-Clark et al., 2010). These events ultimately created the bounding fault complexes for the Loppa High and gave this structural element its general configuration (Brunstad and Rønnevik, 2024). The southern and southwestern parts of the Loppa High were deeply eroded during late Cretaceous and early Paleogene, both through subaerial and submarine processes (Indrevær et al., 2017). Rifting of the North Atlantic during the Paleocene and Eocene reactivated transform fault systems and resulted in the formation of transtensional grabens and transpressional domes, continuing through the Oligocene, decreasing during the Miocene and Pliocene, and ultimately stopping by the Pleistocene (Brunstad and Rønnevik, 2024). A final phase of uplift and erosion occurred during the Pleistocene glaciations, with total uplift and erosion approximately 1500 m since the early Oligocene on the Loppa High area (Cavanagh et al., 2006; Lasabuda et al., 2021; Ktenas et al., 2023).

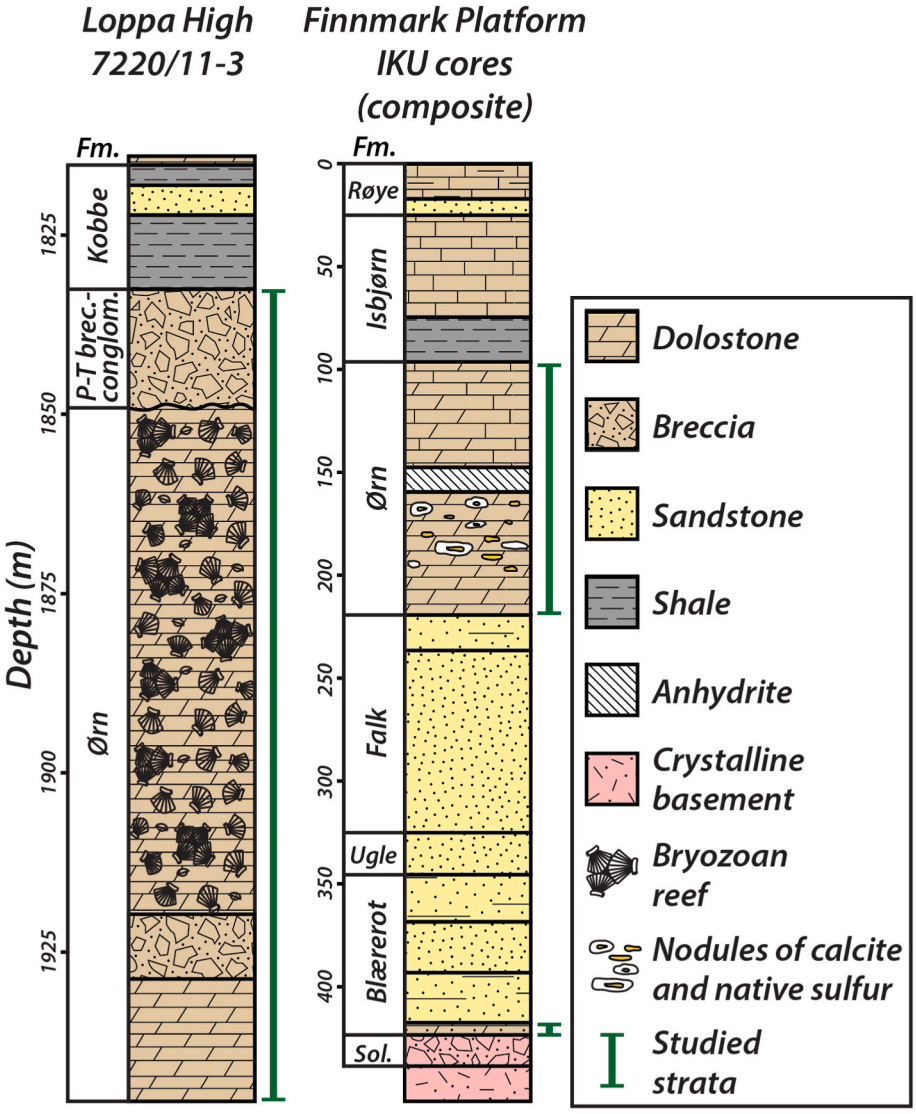

Fig. 2. Simplified stratigraphy of the Loppa High and Finnmark Platform. Well 7220/11-3 was chosen as representative as it is the most heavily sampled core for this study. The stratigraphy of the Finnmark Platform is a composite from wells 7128/12-U-01, 7129/10-U-02, 7030/03-U-01, 7029/03-U-02, and 7029/03-U-01. The sampling bars indicate the approximate range of stratigraphy that was studied from all drill cores combined, rather than a single core.

2.2. Finnmark Platform

The Finnmark Platform structural element contains sedimentary rocks deposited from the Lower Carboniferous to the Paleocene (Henriksen et al., 2024). Rifting occurred in the late Mississippian to early Pennsylvanian along reactivated faults within the crystalline basement, and mafic intrusions were emplaced during this time, with $^{40}Ar/^{39}Ar$ ages of 340 ± 4 and 337.3 ± 0.4 Ma (Lippard and Prestvik, 1997). The Finnmark Platform was tectonically inactive from the upper Carboniferous through the Permian (Henriksen et al., 2024). Minor domal features observed in seismic sections of Triassic sediments may be the result of compressive forces during the Uralian Orogeny (Müller et al., 2019). Minor rifting occurred during the Upper Jurassic to Lower Cretaceous, followed by significant uplift and erosion occurred during the Cenozoic, due to opening of the Atlantic Ocean reactivating Mesozoic fault systems (Henriksen et al., 2024; Lasabuda et al., 2021). Approximately 1200 m of erosion occurred during the Pliocene-Pleistocene glaciations, exposing bedrock outcrops along the seafloor (Cavanagh et al., 2006; Ktenas et al., 2023).

2.3. Studied Lithostratigraphic units

2.3.1. Blærerot Formation

The Blærerot Formation was studied only in IKU drill core 7029/03-U-01 from the Finnmark Platform (Fig. 2). It is the oldest unit studied here, with palynological studies indicating deposition during the Viséan to Serpukhovian ages of the Carboniferous Period (ca. 347–323 Ma; Bugge et al., 1995; Lopes et al., 2018). The following description is based on the observations and interpretations of Larssen et al. (2002). The base of this formation consists of several meters of partially dolomitized bioturbated limestone with abundant bioclasts interpreted to represent an initial marine transgression. Overlying this are a few tens of meters of siliciclastic deposits comprised of coarsening upward silty shale and two siltstone-sandstone coarsening-upward packages with trough cross bedding and wave ripples, cumulatively interpreted to represent deposition in a lower shoreface to upper shoreface transition and potentially fluvial environments. As a whole, the formation records deltaic and/or shoreface progradation during marine transgression. In the studied area of the Finnmark Platform, this unit is approximately 70 m thick.

2.3.2. Ørn Formation

The Ørn Formation was studied in drill cores from the Loppa High, as well as seafloor samples and IKU drillcore from the Finnmark Platform (Fig. 2). This unit was deposited during the latest Carboniferous to early Permian (Gzelian to Sakmarian stages; ca. 304 to 294 Ma) and is composed largely of dolomite and limestone, with some evaporite intercalations; siliciclastics are comparatively rare. In shallower platform areas the lower part of the formation generally consists of dolomitic mudstone and wackestone, overlain by interbedded *Palaeoaplysina* buildups and bioclastic wackestone, then dolomitic mudstone with nodular anhydrite. These lithofacies have been interpreted to represent deposition in a shallow marine environment and the eventual development of a sabkha (Larssen et al., 2002). The upper part of the formation is composed of foraminifera- and algae-rich packstone and grainstone overlain by rhythmically interbedded shale and crinoid-rich silty dolo-wackestone, passing upwards into foraminifer-rich packstone and grainstone, indicating that deposition occurred during a flooding event (Larssen et al., 2002). Cores 7030/03-U-01 and 7029/03-U-02 contain up to 8 m thick intervals of bedded anhydrite and frequent anhydrite nodules. Anhydrite nodules in core 7029/03-U-02 are locally replaced with native sulfur closely associated with calcite spar (Ehrenberg et al., 2002; Hodgskiss et al., 2022). In deeper areas on the distal ramp and in the basin, the lower part of the Ørn Formation consists of dolomitic mudstone and packstone interbedded with massive anhydrite that increases in proportion upward, and is in turn overlain by rhythmically interbedded calcareous shale and fossiliferous limestone with chert nodules (Larssen et al., 2002). On the Loppa High, the presence of bryozoan reefs with abundant fibrous, early-marine cements is established from cored wells. Thicknesses of several tens of meters have been drilled and stacked buildups with a cumulative thickness of several hundreds of meters have been observed in seismic. The reef facies locally contains hydrothermal cements consisting of barite, fluorite and minor sphalerite and galena. The preserved thickness of the Ørn Formation in the studied area on the Loppa High ranges from 0 m, where it has been fully eroded during Permo-Triassic uplift, to approximately 70 m. In the studied drill core from the Finnmark Platform, it has a thickness of approximately 130 m.

2.3.3. Permo-Triassic breccio-conglomerate

The Permo-Triassic Breccio-Conglomerate is an informal stratigraphic unit that unconformably overlies the Ørn Fm and occurs locally around the Loppa High (Fig. 2). It consists of different types of breccia and conglomerate, and is not present on the Finnmark Platform (Brunstad and Rønnevik, 2024; Matysik et al., 2021; Sayago et al., 2012 and references therein). This unit was developed by erosion of as much as 500 m of uplifted Carboniferous and Permian strata (mainly Falk and Ørn formations) and most commonly consists of clasts <10 cm in diameter representing various dolomitized lithofacies. The clasts range from oval to highly irregular and from equidimensional to highly elongated, and are poorly sorted, randomly oriented, and very densely packed. This lithofacies is interpreted to represent lithified colluvium or scree next to a cliff. Other, minor lithofacies within this informal unit are interpreted to have formed from seismic activity. Towards the top of the unit, the continental breccia described above were subject to marine reworking into conglomerate and coarse dolomitic sandstone during the Early Triassic transgression. Interpreted depositional environments include marginal marine, tidally influenced upper shoreface, tidal flats and/or lacustrine shorelines. The thickness of this unit ranges from approximately 0 to 90 m in the studied drill cores.

3. Materials and methods

Samples were collected to be representative of the different carbonate lithologies present (e.g., fossiliferous, micritic) as well as the different types of diagenetic cements, in addition to covering a broad range of stratigraphy. Twenty-four samples were collected from six drill cores on the Loppa High (7220/11-1, 7220/11-2, 7220/11-3, 7220/11-3AT2, 7220/11-4, 7220/11-4A), nineteen from five IKU drill cores of the Finnmark Platform (7029/03-U-01, 7029/03-U-02, 7030/03-U-01, 7128-12-U-01, 7129/10-U-02), and thirty samples from two seafloor outcrops off the Finnmark coast (Fig. 3; approximate coordinates N70.9687°, E29.7361°) using a remotely operated vehicle (ROV). The seafloor outcrops consist of erosion-resistant carbonate units of Ørn Formation at ~350 m water depth occur as the southernmost of two parallel, NW-SE trending, up to 10 m high submarine cliffs ('cuestas'). Massive anhydrite is exposed in a dissolution depression on top of the southern cliff, ~100 m wide and 4 m deep (Fig. 3).

Carbon and oxygen isotope ratios of microdrilled carbonate sample powders were measured at the University of Tartu (Tartu, Estonia), using a Thermo Scientific Delta V Advantage continuous flow isotope ratio mass spectrometer. Analytical uncertainty for $\delta^{13}C$ and $\delta^{18}O$ are both less than ±0.2‰ (2σ). All analyses of $\delta^{13}C$ and $\delta^{18}O$ are reported relative to the Vienna PeeDee Belemnite (VPDB) SRM (standard reference material).

Two sets of parallel thin sections, 30 μm thick and 100 μm thick, were prepared for each sample. The standard 30 μm thin sections were subject to detailed petrographic study to determine the paragenetic sequence of mineral formation for each sample set. Following petrographic characterization, the 100 μm polished thin sections were studied using μXRF (micro X-ray fluorescence) element mapping at NTNU (Norges teknisk-naturvitenskapelige universitet; Trondheim, Norway) to identify different generations of carbonate minerals and variations in

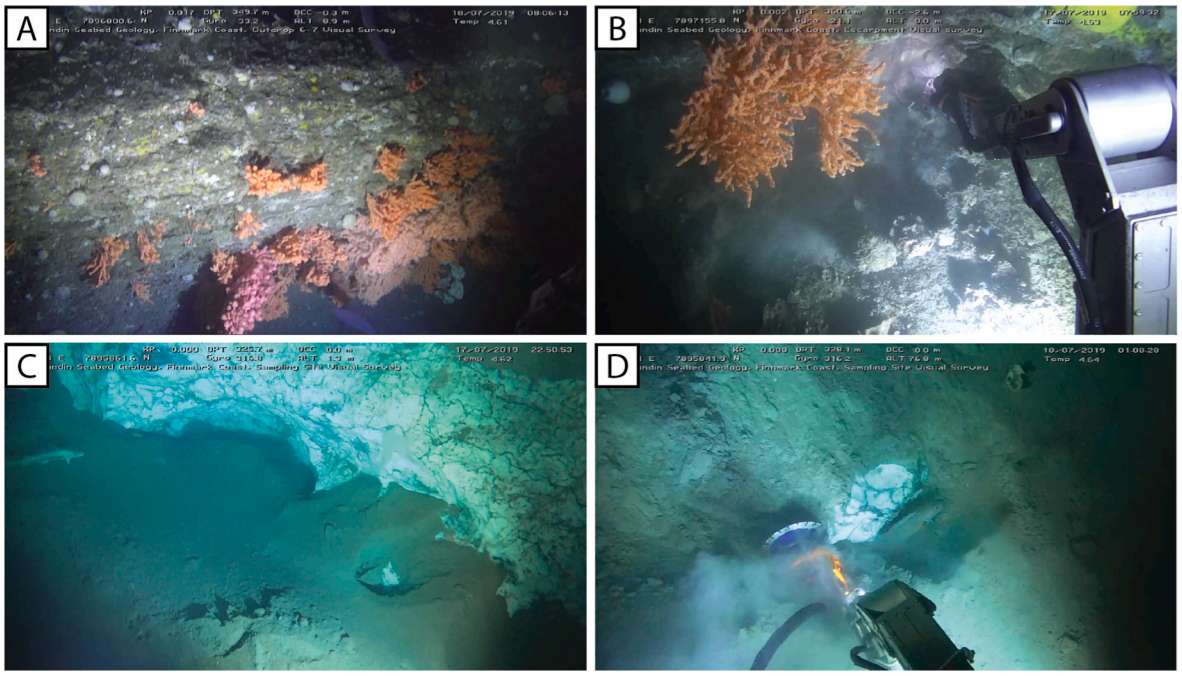

Fig. 3. Seafloor outcrops on the Finnmark Platform. A) Outcropping carbonate lithologies of the Ørn Formation partially overgrown by corals. Identification of this outcrop as belonging to the Ørn Formation required seismic cross sections and study of petrographic thin sections due to poor visibility of outcropping structures and lithologies, although crude bedding is visible oriented approximately horizontal. B) Sampling of the Ørn Formation using the manipulator arm. C) An outcrop of anhydrite from the Ørn Formation. Note the chickenwire-like texture of the massive anhydrite and solutions hollows that suggest ongoing dissolution. D) Sampling of anhydrite evaporite outcropping in the seafloor sinkhole using the manipulator arm and saw. Fields of view are approximately 2 m on all images. No corals or fish were harmed during sample collection.

elemental composition (refer to Supplementary Information). Millimetre-sized areas of selected thin sections were screened using a laser ablation (LA) system with an inductively coupled plasma mass spectrometer (ICP-MS) at the University of Tartu and Geological Survey of Norway (NGU; Trondheim, Norway) to determine U and Pb content, as well as Al, Th, and Ti to screen for silicate mineral contamination. Areas of interest several mm^2 containing elevated U contents potentially suitable for U–Pb dating were then mapped in high resolution using LA-ICP-MS. U–Pb isotopic analyses were carried out at NGU using a LA system coupled to a multi collector ICP-MS, and a LA system coupled to a single collector ICP-MS at the British Geological Survey (Nottingham, United Kingdom) following Roberts et al. (2017). Laser spot sizes of 45 and 80 μm were used depending on the size of the target, and WC-1, Duff Brown, and NIST 614 were used as SRMs (Hill et al., 2016; Roberts et al., 2017). LA-ICP-MS mapping data and U–Pb geochronological data were reduced using the Iolite 4 software package (Paton et al., 2011; Petrus et al., 2017), with final ages and Tera-Wasserburg diagrams created using model-3 fitting in IsoplotR (Vermeesch, 2018). An additional 2.5% error was quadratically added to all final age results to account for the uncertainty in WC-1 (Roberts et al., 2017), and all ages are reported with 2σ uncertainties. Additional details for analytical methods are reported in the Supplementary Information.

Basin modelling was performed using the Trinity software from ZetaWare Inc. Regional depth maps, based on seismic interpretations, were used as the input for thermal modelling, and borehole temperature data was extracted from exploration wells in the area. Burial/temperature history was constructed using regional depth maps from regional seismic interpretation done by Lundin Energy Norway (now part of AkerBP ASA). A constant geothermal gradient of 35°C/km was used, calculated from exploration well data available from the Norwegian Petroleum Directorate fact pages (npd.no). Net erosion was estimated from vitrinite reflection versus depth trends. A one-dimensional temperature-time model was constructed to represent the thermal evolution, and the main uncertainties in this approach are the maximum burial depths of the stratigraphy and variations in subsurface paleotemperatures through time. Therefore, results from the thermal modelling should be treated more as approximations of the temperatures and event timing, rather than accurate statements of the temperatures. Burial history modelling was conducted without input from U–Pb geochronological results.

4. Results

4.1. Textural relationships and paragenesis

For each of the studied formations on the Loppa High and the Finnmark Platform, brief summaries of their diagenetic evolution are presented below and summarized in Fig. 4, with detailed descriptions presented in the Supplementary Information.

In the Ørn Formation on the Loppa High, diagenetic processes were chiefly comprised of early-marine cementation, dolomitization, silicification, and late calcite cementation. Dolomitization was the main diagenetic process, as fabric-preserving crypto- and fine-crystalline dolomite is observed to pervasively replace grains, micrite, and early-marine cements in all samples. This process most likely also resulted in dissolution of bioclasts and creation of abundant non-selective dissolution vugs throughout the succession. Many interparticle pores, molds, cracks, dissolution vugs, and interclast spaces are partly to completely cemented with late stage poikilotopic calcite.

Diagenetic processes in the P-T breccio-conglomerate unit mainly include dolomitization of interstitial micrite and later precipitation of various cements in interclast spaces and fractures. Cements within the interclast spaces can be composed of isolated coarse dolorhombs, isolated megaquartz crystals with inclusions of precursor sediments, and authigenic quartz overgrowths around detrital quartz grains. Later cements include pyrite, sphalerite, barite, fluorite, and poikilotopic calcite as the last cement phase.

In the Blærerot Formation on the Finnmark Platform, micrite was

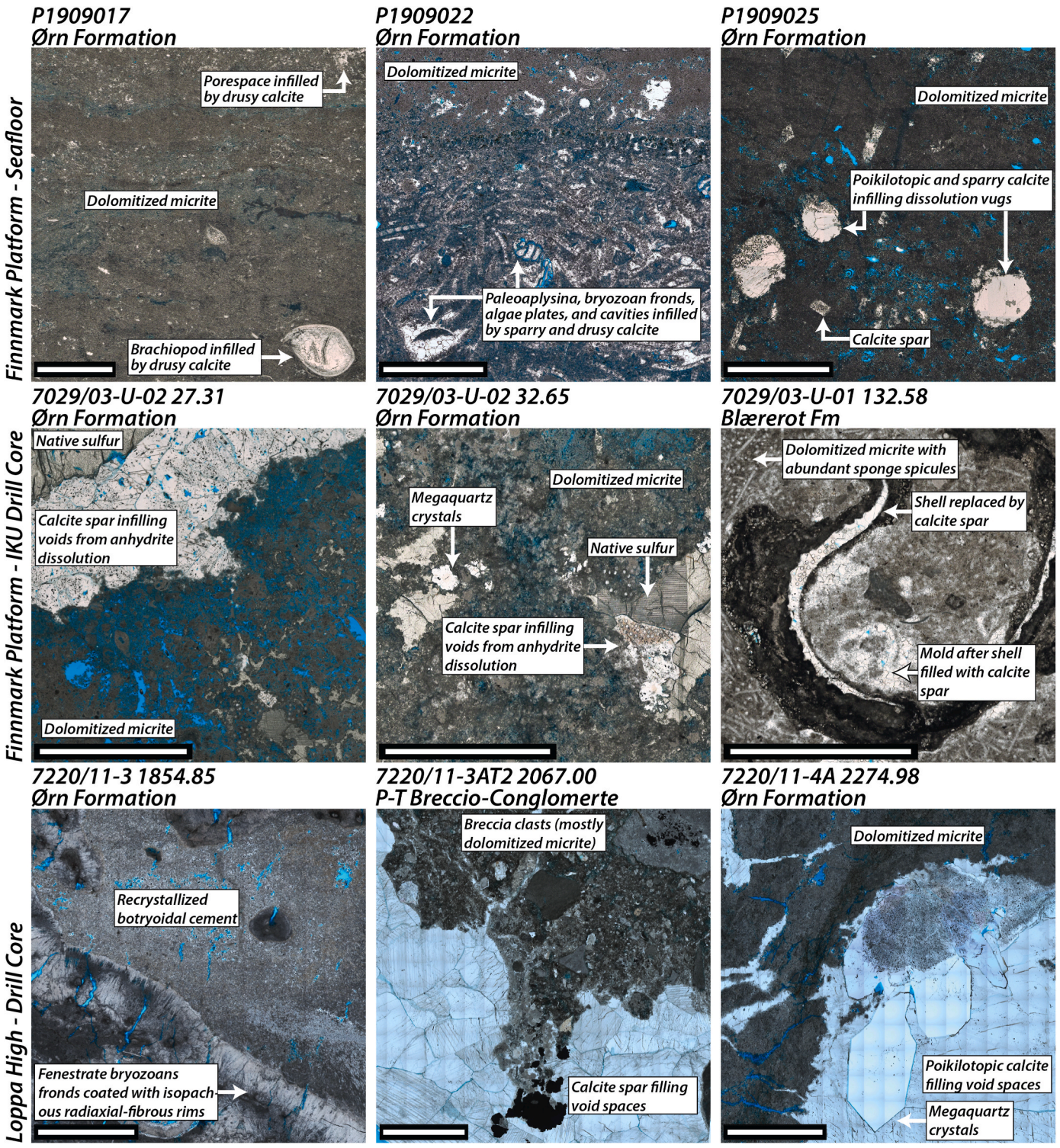

Fig. 4. Representative photomicrographs of analyzed samples. All scale bars are 5 mm wide.

recrystallized to microspar, and subsequently dolomitized; some void spaces after bioclasts contain rhombic dolomite crystals up to 1 mm across. Dissolution of spicules and bivalves/gastropods occurred early, and these cavities, as well as oncoid nuclei and cortices, are filled by drusy calcite, calcite spar, and poikilotopic calcite.

The paragenetic sequence of the Ørn Formation on the Finnmark Platform is characterized primarily by dissolution, dolomitization, and calcite cementation, with minor amounts of silicification, fracturing, chemical compaction, precipitation of accessory minerals, and oil staining. Dissolution is manifested as molds after bioclasts, vugs in micrite, and voids in megaquartz. Dolomitization is common but affects only micrite, which ranges from undolomitized to pervasively dolomitized. Four types of calcite cement form rims and fill void spaces, particularly in bioclast molds and fractures. Native sulfur is primarily associated with variously silicified and calcite-replaced anhydrite nodules. Samples of the Ørn Formation are very similar between IKU drill core 7029/03-U-02 and the seafloor samples, the primary difference being the occurrence of native sulfur in the former.

4.2. Sample screening and geochronological results

Of the 73 samples collected, 22 were suitable for dating. Samples were primarily eliminated because of either insufficient U concentrations or excessive contamination by siliciclastic minerals. Results are summarized briefly here and detailed in Table 1.

On the Loppa High, ages for Ørn Formation dolomicrite range from approximately 380 to 310 Ma, and three sparry calcite cements within the Ørn Formation record ages from approximately 75 to 45 Ma (Fig. 5). Micrite clasts within the P-T breccio-conglomerate range in age from approximately 415 to 260 Ma, while two samples of poikilotopic calcite cement filling intraclast pores yielded ages of approximately 240 Ma (Fig. 6). On the Finnmark Platform, a sample of the Blærerot Formation yielded an age for dolomite rhombs of 380 Ma, 342 Ma for a bioclast, and 337 Ma for dolomicrite (Fig. 7). Finally, seafloor samples yielded Ørn Formation dolomicrite ages from 350 to 260 Ma, and two samples of poikilotopic calcite cement within the Ørn Formation formed approximately 100 Ma (Fig. 8).

4.3. Carbon and oxygen isotope ratios

On the Loppa High, carbon and oxygen isotope ratios analyses were

Table 1
Summary of carbonate U–Pb geochronological results.

Well	Sample	Formation	Petrographic description	Age (Ma)	Propagated uncertainty	MSWD	$^{207/206}Pb_i$ (±2σ)	N/N
Loppa High								
7220/11-4A	2262.43	Ørn	Large, clear calcite crystals filling void space.	74.2	12.7	1.9	0.877 ± 0.035	29/32
			Dolomicrite matrix.	358.5	14.6	3.0	0.833 ± 0.012	46/46
	2274.98	Ørn	Large, clear calcite crystals filling void space.	59.1	1.6	1.4	0.858 ± 0.010	33/34
			Dolomicrite matrix.	344.3	19.5	1.6	0.863 ± 0.005	45/45
7220/11-3AT2	2067.00	P-Tr Breccio-conglomerate	Dolomicrite clast	254.1	56.2	1.5	0.851 ± 0.006	38/38
			Poikilotopic calcite	246.2	8.9	1.6	0.859 ± 0.002	46/49
	2093.84	P-Tr Breccio-conglomerate	Dolomicrite matrix.	347.7	24.6	0.64	0.858 ± 0.004	50/50
	2075.77	Ørn	Dolomicrite matrix	315.5	18.9	1.7	0.856 ± 0.003	70/70
7220/11-4	1966.70	Ørn	Dolomicrite breccia clasts	414.2	83.5	1.9	0.869 ± 0.005	30/30
			Dolomicrite breccia clasts	378.5	27.7	1.6	0.867 ± 0.004	50/50
7220/11-3	1854.85	Ørn	Fibrous cement	329.0	38.2	1.2	0.863 ± 0.006	31/31
			Dolomicrite	320.7	13.7	0.97	0.869 ± 0.006	30/30
	1931.78	Ørn	Dolomicrite matrix	333.0	30.5	1.2	0.864 ± 0.002	82/82
	1932.42	Ørn	Dolomicrite matrix.	314.8	36.8	1.2	0.859 ± 0.006	40/40
	1937.77	Ørn	Dolomicrite matrix.	310.1	63.1	0.85	0.863 ± 0.004	39/39
			Large, clear calcite crystals filling void space.	46.5	16.4	3.4	0.853 ± 0.003	38/42
7220/11-2	1920.76	P-Tr Breccio-conglomerate	Coarse calcite spar between clasts in P-T breccio conglomerate	238.7	8.1	2.8	0.827 ± 0.003	43/47
Finnmark Platform – IKU Cores								
7029/03-U-01	132.58	Blærerot	Bioclast	342.1	9.0	1.3	0.92 ± 0.24	15/15
			Bioclast replacement	333.0	61.5	4.7	0.783 ± 0.006	24/25
			Dolomicrite	337.1	13.5	3.8	0.816 ± 0.028	19/21
			Dolomite rhombs	363.4	27.2	4.7	0.786 ± 0.011	11/12
Finnmark Platform – Seafloor samples								
–	1909029	Ørn	dolomicrite/finely crystalline dolomite	279.8	50.2	8.7	0.714 ± 0.017	17/17
	1909025	Ørn	dolomicrite	299.5	14.2	5.4	0.706 ± 0.019	25/26
	1909025	Ørn	molds, porespaces, fractures, and dissolution vugs filled by coarse calcite spar and poikilotopic calcite	99.6	3.1	5.2	0.692 ± 0.008	22/22
	1909022	Ørn	Dolomicrite	285.0	30.1	3.0	0.787 ± 0.028	10/10
	1909017	Ørn	Dolomicrite	302.9	21.5	9.6	0.738 ± 0.023	15/18
	1909015	Ørn	Dolomicrite	266.3	17.6	9.5	0.626 ± 0.018	18/18
	1909015	Ørn	Poikilotopic calcite filling fractures and dissolution vugs	95.7	2.9	13.0	0.645 ± 0.008	14/18

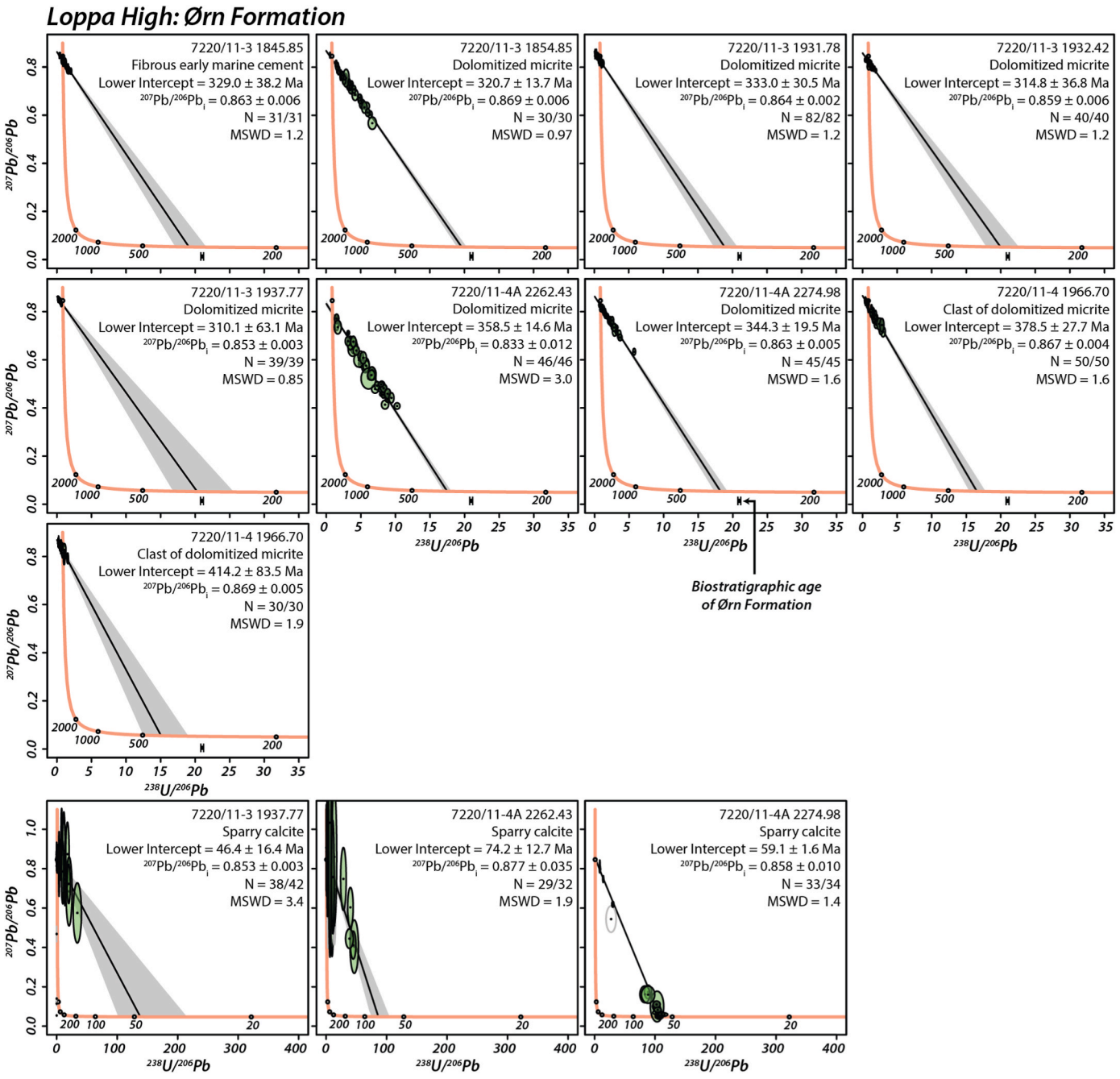

Fig. 5. Tera-Wasserburg diagrams for Ørn Formation samples from the Loppa High. Dolomicrite samples record ages of ca. 415 to 310 Ma, compared to ca. 75 to 45 Ma for calcite spar.

carried out on samples from the Falk and Ørn formations and the overlying Permo-Triassic breccio-conglomerate (Fig. 9). The $\delta^{13}C$ and $\delta^{18}O$ values of Ørn Formation dolomicrite (N = 27) range from +1.9‰ to +5.6‰ and −4.3‰ to +1.1‰, respectively. Poikilotopic calcite (N = 5) within the Ørn Formation records a range in $\delta^{13}C$ values from +0.4‰ to +2.6‰, and a range in $\delta^{18}O$ values from −11.3‰ to −6.8‰. Samples from the underlying Falk Formation (N = 8) span a similar range for $\delta^{13}C$ (+2.7‰ to +4.5‰) and $\delta^{18}O$ (−6.0‰ to −1.5‰). Isotopic results for dolomicrite clasts from the Permo-Triassic breccio-conglomerate (N = 16) are similar to the Ørn and Falk formations from which the clasts were derived, with $\delta^{13}C$ ranging from +0.7‰ to +5.5‰ and $\delta^{18}O$ ranging from −6.2‰ to +1.9‰. Poikilotopic calcite cement from the P-T breccio-conglomerate (N = 3) has $\delta^{13}C$ and $\delta^{18}O$ values ranging from −7.4‰ to −1.2‰ and −7.2‰ to −6.3‰, respectively. Calcite spar samples from the P-T breccio-conglomerate (N = 2) have $\delta^{13}C$ values of −6.9‰ and −6.3‰, and $\delta^{18}O$ values of −7.5‰ and −6.9‰.

Analyses of dolomicrite from the Ørn Formation on the Finnmark Platform seafloor (N = 33) form a relatively linear array with positive covariation between C- and O-isotopes. The $\delta^{13}C$ values of these samples range from −2.4 to +4.6‰, and $\delta^{18}O$ ranges from −5.1 to +3.6‰. Analyses of poikilotopic calcite (N = 28) partly overlap with the dolomicrite samples, and have $\delta^{13}C$ ranging from −15.4 to +3.9‰, and $\delta^{18}O$ ranging from −8.3 to 0.0‰.

4.4. Burial history

The modelled burial history is very different between the two studied regions; whereas the western Barents Sea was affected by repeated

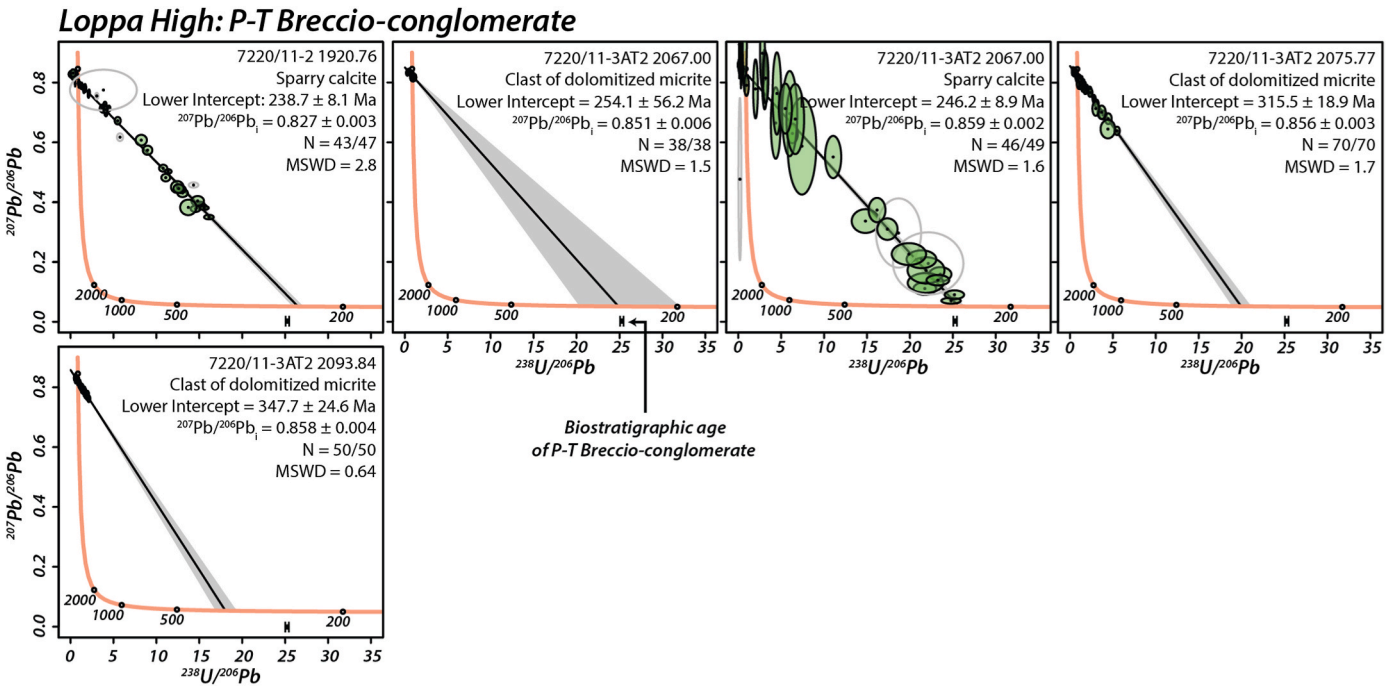

Fig. 6. Tera-Wasserburg diagrams for P-T breccio-conglomerate samples from the Loppa High. Dolomitized clasts range in age from ca. 350 to 250 Ma, and sparry calcite cement within the clasts precipitated ca. 245 to 240 Ma.

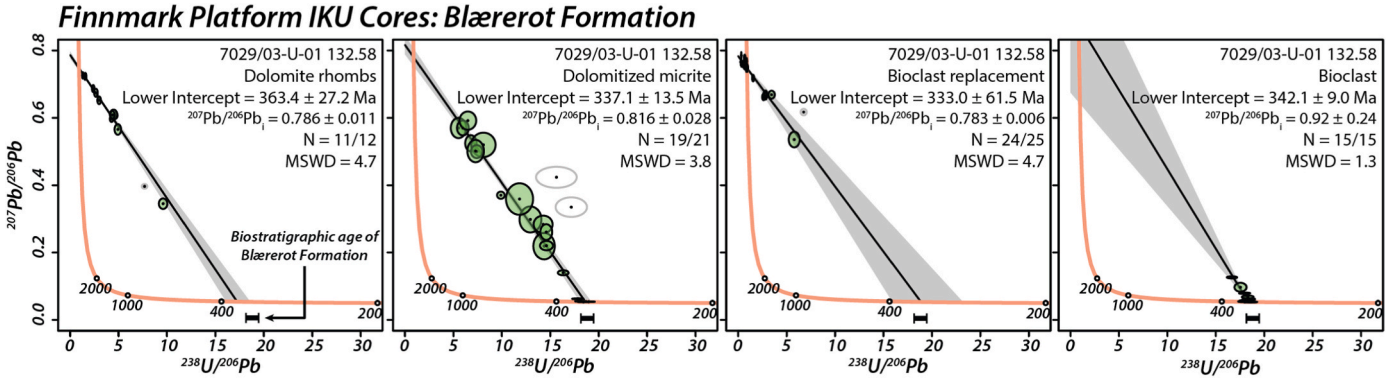

Fig. 7. Tera-Wasserburg diagrams for samples from IKU drill cores. Dolomitization of the Blærerot Formation occurred early, within the biostratigraphic age range. Dolomicrite in the Ørn Formation records ages between ca. 340 to 315 Ma, whereas calcite spar in the Ørn Formation may have formed ca. 50 to 15 Ma.

rifting events (Devonian and Carboniferous, Permian and Triassic, Jurassic and Cretaceous), the Finnmark platform was influenced by the formation of the Nordkapp basin in the Devonian and Carboniferous (Figs. 10 and 11; Brunstad and Rønnevik, 2024; Henriksen et al., 2024). The burial history of the Loppa High will have varied across the structural element due to differential uplift/erosion, and well 7220/11-3 was chosen as representative of the sample set because most samples are from this core, although the other studied drill cores will record broadly similar histories. Following deposition of the Ørn Formation, sediments underwent burial of ~1500 m until around the P-T boundary, when they were rapidly uplifted to within a few hundred meters of the surface. A second burial phase then commenced and lasted to near the Jurassic-Cretaceous boundary, reaching a maximum burial depth of ~2500 m. Uplift of ~1400 m took place over several tens of millions of years, followed by relatively stable conditions that persisted until the Cretaceous-Paleogene boundary. A third burial phase lasted until the late Paleogene, reaching a maximum depth of ~2100 m. This was followed by a final rapid uplift and burial phase during the late Paleogene-Neogene and Quaternary periods, both by ~500 m each.

Well 7029/03-U-02 on the Finnmark Platform (Fig. 11) underwent a comparatively simple burial history, with rapid burial during the Carboniferous and Permian resulting in a maximum depth of ~1300 m by the early-mid Triassic. This was followed by tens of millions of years of stability, until a small burial event in the late Jurassic, followed by a large and rapid burial and uplift event of >1600 m during the Paleogene and Neogene.

5. Discussion

5.1. Challenges of carbonate U–Pb geochronology

Obtaining high-quality carbonate U–Pb geochronological results requires that the carbonate mineral(s) of interest behaved as a closed isotopic system, that they record enough variation in parent/daughter isotope ratios for robust regression fitting, and that the initial common lead composition remained constant during precipitation (Drost et al., 2018; Roberts et al., 2020). In practice, low uranium concentrations and/or high common lead concentrations are often the limiting factor

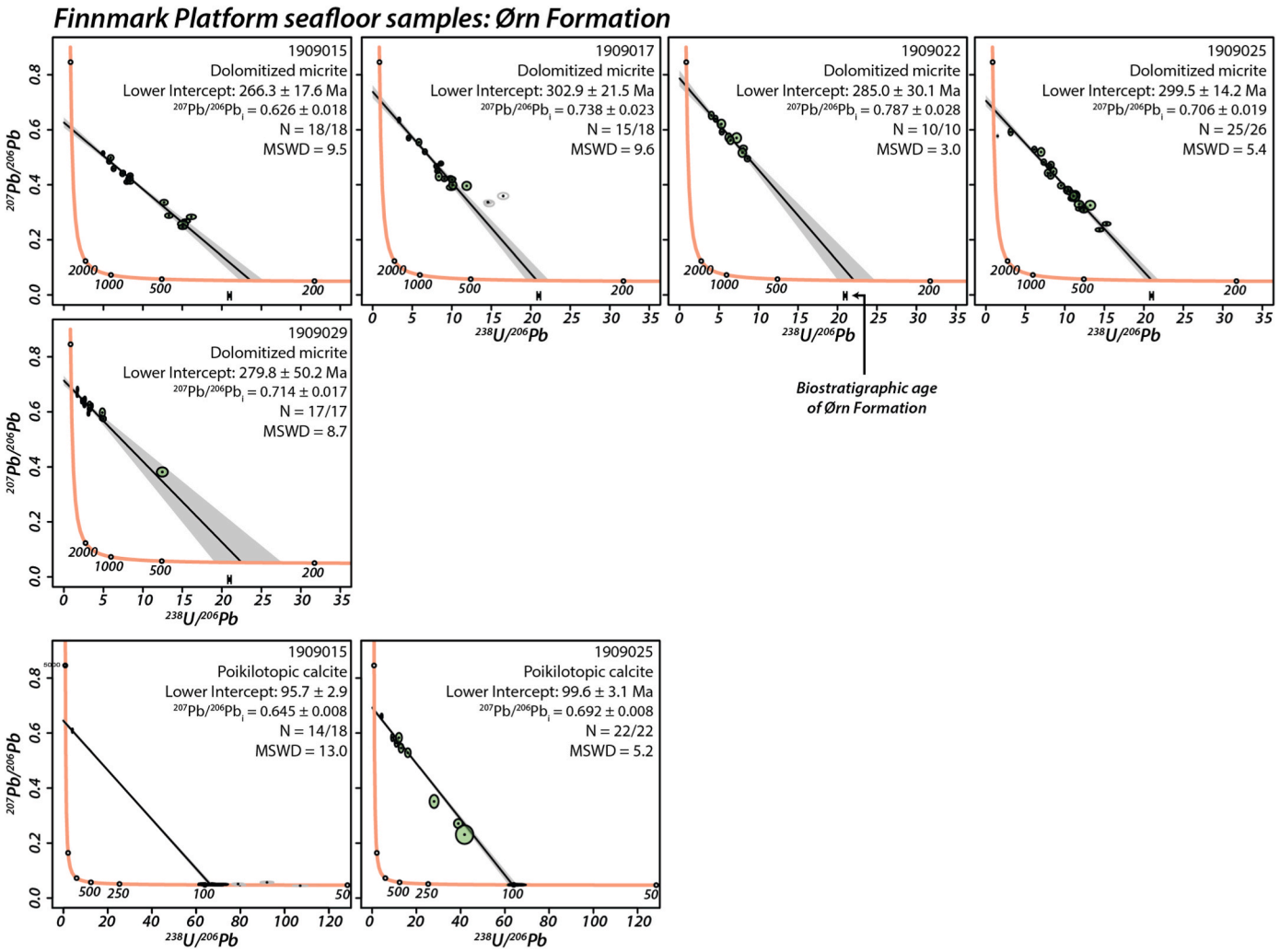

Fig. 8. Tera-Wasserburg diagrams for seafloor samples from the Finnmark Platform. Dolomicrite from the Ørn Formation records ages of ca. 300 to 265 Ma, in contrast to sparry calcite that formed ca. 100 Ma.

for producing high-quality ages (Roberts et al., 2020).

In the studied samples, U concentrations were particularly low in dolomitized micrite samples (Figs. 5–8), resulting in very low $^{238}U/^{206}Pb$ ratios and large lower intercept uncertainties. Another factor of note for the dolomitized micrite samples is the possibility of siliciclastic impurities within the original carbonate sediment, such as clay minerals, that would be ablated during analyses. In contrast, this is less likely to impact calcite cements and spars that are typically free of such impurities. Open system behavior appears to have impacted the analyzed samples to varying degrees, as shown by the differing amounts of scatter observed. While analyses from most samples fall along well-defined discordia lines and have MSWDs relatively close to 1 (mostly between 0.6 and 2.0), some samples exhibit relatively large amounts of scatter in data and high MSWDs, particularly calcite samples from the Finnmark Platform seafloor and IKU drill core (Figs. 7 and 8). This could represent open system behavior, precipitation of cements over long time intervals, or mixing of different age domains, all of which will be discussed in detail later.

5.2. Carbonate U–Pb dating for constraining the age of sedimentation

Both the Blærerot and Ørn formations are biostratigraphically well-constrained, allowing for an independent assessment of whether dolomitization of the micritic sediment occurred early or late. The Blærerot Formation is biostratigraphically constrained to ca. 347–323 Ma (Larssen et al., 2002; Cohen et al., 2013; Lopes et al., 2018), consistent with a measured bioclast age of 342.1 ± 9.0 Ma, and the single measured age of dolomitized micrite (337.1 ± 13.5 Ma) suggests that dolomitization occurred early. The ca. 304 to 294 Ma Ørn Formation (Larssen et al., 2005) yielded a wide range of ages from dolomitized micrite that only broadly overlap with the accepted biostratigraphic ages. In samples from the Loppa High, the measured ages range from 358.5 to 310.1 Ma, and on the Finnmark Platform, the measured ages range from 338.0 to 266.3 Ma. Of the seven dolomitized micrite samples analyzed from the Loppa High, all seven yielded ages older than the biostratigraphic age, potentially indicating the dolomitization occurred very early. In contrast to the Loppa High, all five analyzed samples of dolomitized micrite from the Finnmark Platform overlap with or post-date the biostratigraphic age, potentially indicating that dolomitization occurred later than on the Loppa High. Further, these dolomite analyses generally have large uncertainties, ranging from 14 to 63 Myr (median of 20 Myr) and only approximate the accepted biostratigraphic ages for the Ørn Formation.

It is interesting to note that the initial $^{207/206}Pb$ varies regionally (Table 1), with samples from the Loppa High recording values that cluster very closely around 0.86, close to the $^{207}Pb/^{206}Pb$ composition of Holocene sediments (~0.83; Pinedo-González et al., 2018). In contrast, samples from the Finnmark Platform are variable but typically more radiogenic (i.e., lower values), with all samples except one between 0.63 and 0.82. One possibility is that sediments deposited on the Loppa High

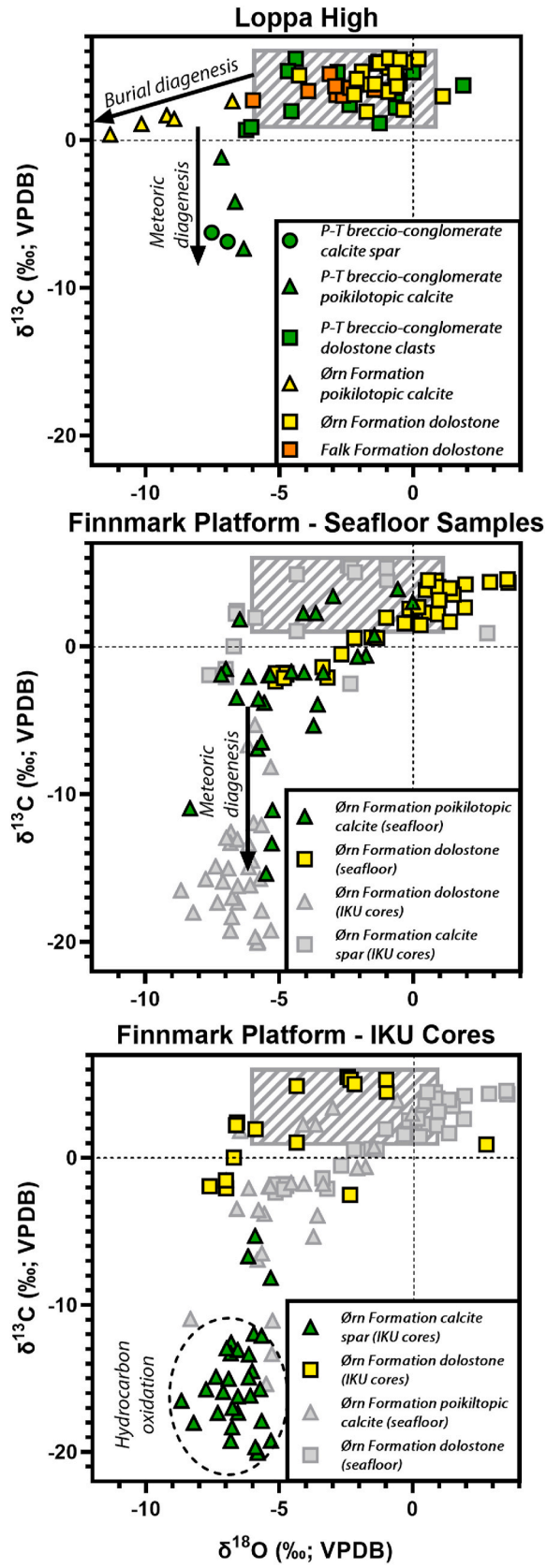

(caption on next column)

Fig. 9. Carbon and oxygen isotope ratio systematics from the Loppa High and Finnmark Platform. Samples from the Loppa High form three distinct populations: dolostone from the Ørn and Falk formations fall within the field of contemporaneous seawater (grey box), as do clasts of the aforementioned formations in the P-T breccio-conglomerate. Poikilotopic calcite within the Ørn Formation records strong covariation between $\delta^{13}C$ and $\delta^{18}O$, and a burial diagenesis trend, whereas poikilotopic and sparry calcite in the P-T breccio-conglomerate record strongly negative $\delta^{13}C$ values with minimal variation in $\delta^{18}O$, consistent with a meteoric diagenesis trend. Samples of dolomite and calcite from the Finnmark Platform seafloor strongly overlap, and are interpreted to represent a mixing array between calcite and dolomite endmembers during microdrilling rather than a primarily diagenetic trend. The vertical array formed by calcite is interpreted to represent a meteoric diagenesis trend, and is distinct from the C–O isotope trend recorded by hydrocarbon-derived calcite spar in the IKU drill core (Hodgskiss et al., 2022).

underwent seawater-buffered early diagenesis, whereas sediments deposited on the Finnmark Platform underwent early diagenesis with a distinctly non-seawater-like diagenetic fluid, potentially sourced from the underlying Archean crystalline 'basement' rocks. Thus, the Pb isotopic composition of these dolomicrite samples may indicate that they underwent different styles of early diagenesis, potentially explaining the regional variability in their ages. A second noteworthy feature of the dolomicrite data are their large uncertainties and potentially low accuracies (i.e. measured ages older than the biostratigraphic age). While the reasons behind this are difficult to ascertain, a primary factor is likely the low initial U/Pb ratios providing measurements dominated by initial (i.e. common) rather than radiogenic lead, and low variability in measured U/Pb ratios. However, several other factors can be speculated. The first is the lack of a dolomite standard reference material (SRM), with only calcite SRMs available for calibration of U–Pb geochronology, resulting in mismatched matrices. A consequence of this may be different ablation characteristics between dolomite samples and calcite SRMS. Guillong et al. (2020) demonstrated that dolomite can be ablated up to 60% more efficiently than calcite and exhibits significantly more variability in ablation rates, potentially resulting in a 4–8% offset in calculated ages; although notably their study only compared a small number of dolomitic samples with calcite. This bias would correspond to offsets of approximately 12–24 million years in the Ørn Formation, and would encompass almost all measured dolomicrite ages from the Loppa High. Regardless of this potential offset, many studies have proceeded with dolomite U–Pb, with the general assumption that the measured results are likely to be accurate within the stated uncertainties (e.g. Pan et al., 2020, 2021; Su et al., 2020, 2022; Rochelle-Bates et al., 2021, 2022; Xiong et al., 2023; Zhang et al., 2023). Conversely, Elisha et al. (2021) suggested that differences in ablation efficiency may not be a controlling factor, and instead suggested that factors such as intracrystalline porosity, carbonate grain size, and zoning may be more important, as they can result in ablation of minerals such as sulfides, oxides, or clays with different U–Pb compositions, and mixing of age domains. While it is beyond the scope of this study to determine which factors are most important, the analyzed dolomicrite samples are heterogeneous both in optical microscopy and μXRF element mapping, some degree of mineral/age domain mixing undoubtedly occurred, and possibly some component of the dolomicrite was sourced from recycling/redeposition of older sedimentary rocks deposited on the Loppa High. More generally, these results urge caution against assuming all carbonate dates provide accurate constraints on depositional ages, particularly when studying heterogeneous materials with high common Pb concentrations.

5.3. Stable isotope systematics

On the Loppa High, the $\delta^{13}C$ and $\delta^{18}O$ ratios of dolomitized micrite from the Falk and Ørn formations (Fig. 9) are consistent with the isotopic composition of seawater during the Pennsylvanian and Permian (e.

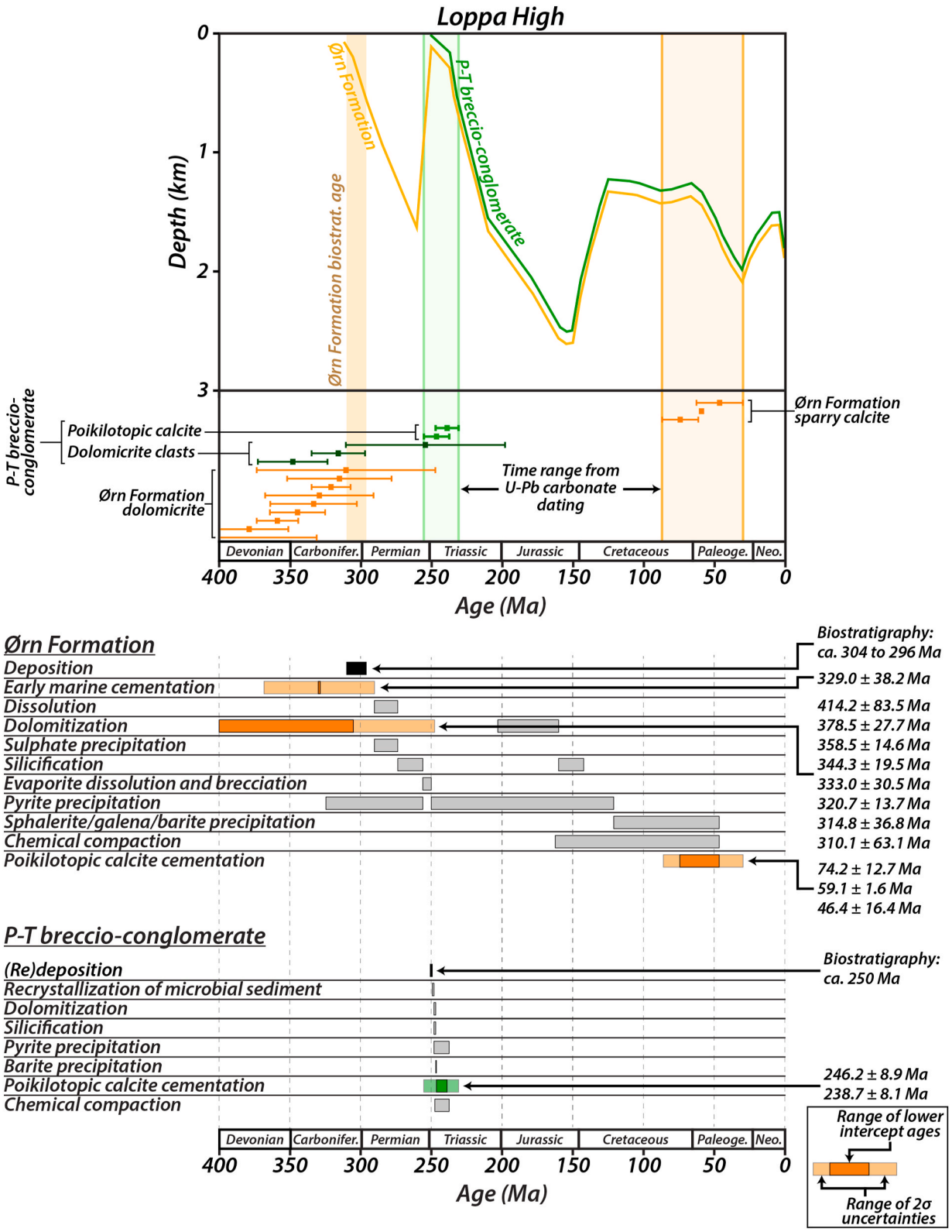

Fig. 10. Comparison of modelled burial histories with measured carbonate U-ages for the Loppa High. This region records a more complex burial history marked by several rapid phases of uplift and burial, two of which are greater than 1500 m. Dolomicrite in the Ørn Formation and clasts in the P-T breccio-conglomerate are generally older than the accepted biostratigraphic ages and only approximate the timing of deposition Poikilotopic calcite within the P-T breccio-conglomerate precipitated during the early phase of burial, whereas calcite spar in the underlying Ørn Formation precipitated during a much later burial event. Colored bars correspond to phases that were dated using in-situ U–Pb geochronology, black bars correspond to biostratigraphic age constraints, and grey bars to events that are undated and only constrained relative to other events through petrography.

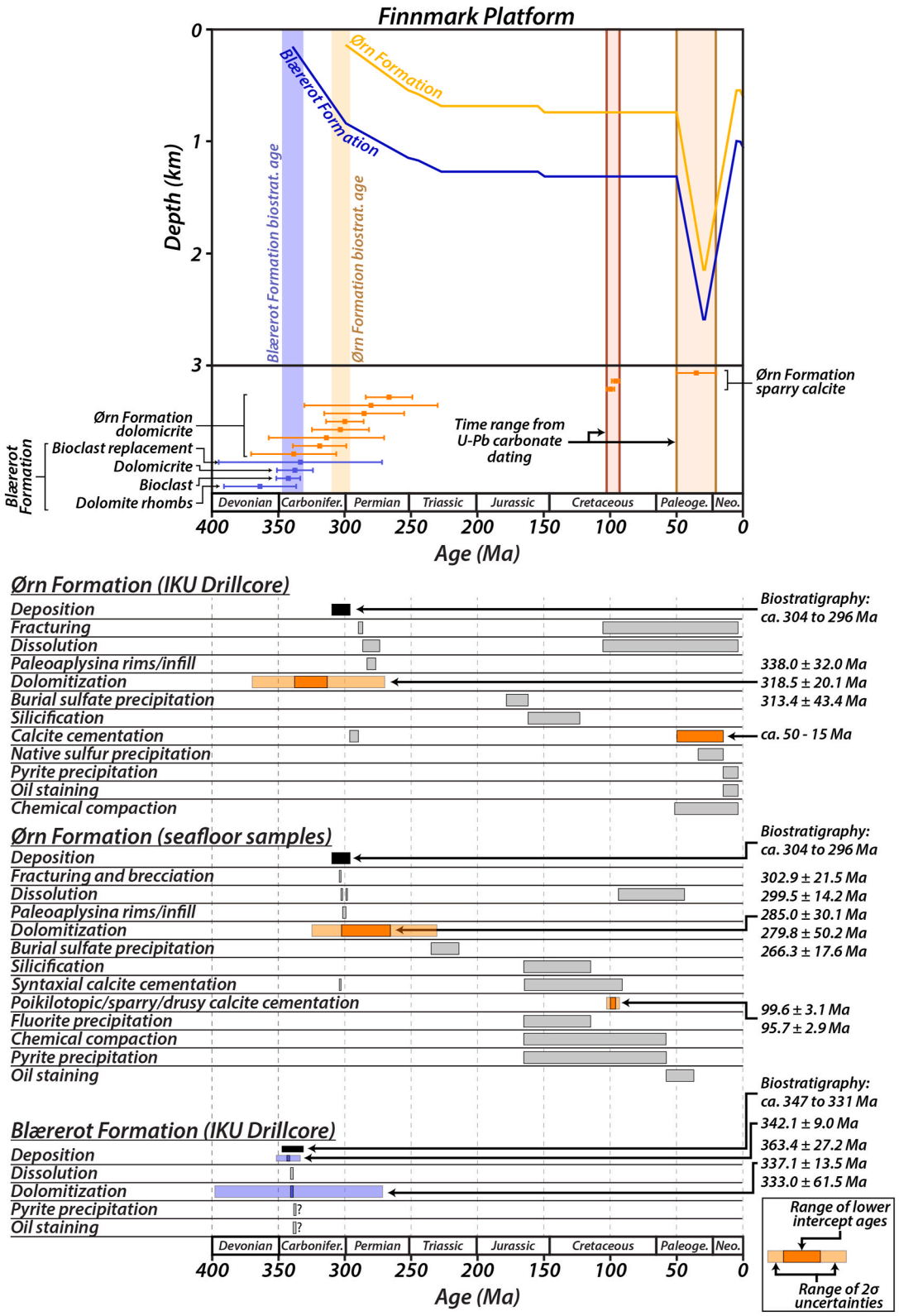

Fig. 11. Comparison of modelled burial history and carbonate U–Pb ages for the Finnmark Platform. This region records a relatively simple history marked by gradual burial in the Carboniferous through Triassic, and a single rapid period of burial and uplift in the Paleogene-Neogene. Analyses of a bioclast and dolomicrite in the Blærerot Formation agree well with the biostratigraphic age of the formation, whereas measured ages for the Ørn Formation span a wide range and only broadly agree with the biostratigraphic age. Calcite that precipitated ca. 100 Ma in the seafloor samples is not associated with any modelled change in the burial history, and may be related to emplacement of the High Arctic Large Igneous Province. In contrast, calcite spar from the IKU cores that formed ca. 50 to 15 Ma may be related to the migration and oxidation of hydrocarbons during burial and uplift (Hodgskiss et al., 2022). Colored bars correspond to phases that were dated using in-situ U–Pb geochronology, black bars correspond to biostratigraphic age constraints, and grey bars to events that are undated and only constrained relative to other events through petrography.

g., Buggisch et al., 2011), indicating that dolomitization took place during early diagenesis while the sediments were buffered by seawater rather than burial or meteoric fluids with 'evolved' compositions. Analyzed clasts of the P-T breccio-conglomerate record a similar range of $\delta^{13}C$ and $\delta^{18}O$ values as their Falk and Ørn formation sources (Fig. 9), indicating that alteration was minimal, or at least took place in contact with fluids with C and O isotopic compositions similar to seawater. Poikilotopic calcite within the Ørn Formation records covarying $\delta^{13}C$ and $\delta^{18}O$ ratios, with lower $\delta^{13}C$ values corresponding to lower $\delta^{18}O$ ratios. This is interpreted to represent both increased temperatures and evolving redox conditions of pore fluids during progressive burial during the Cretaceous to Paleogene, resulting in progressively more carbon sourced from the oxidation of organic matter and stronger fractionation of O isotopes during precipitation of calcite (Bojanowski et al., 2014; Liu et al., 2017). Finally, the poikilotopic and sparry calcite in the P-T breccio-conglomerate fall along a vertical array with $\delta^{13}C$ decreasing by more than 7‰ while $\delta^{18}O$ remains near-constant, between −6.3‰ and −7.5‰ (Fig. 9). A relatively large range of $\delta^{13}C$ values for the poikilotopic and sparry calcite can be explained by mixing in the diagenetic realm between host rock carbon (+4‰) and oxidized organic carbon sourced from organic matter, coal, or hydrocarbons. Overall, the C–O isotope systematics of cements in the P-T breccio-conglomerate are consistent with formation during meteoric diagenesis, where the oxidized organic matter with very negative $\delta^{13}C$ values was incorporated into precipitating poikilotopic calcite (e.g., Lohmann, 1988).

In seafloor samples from the Finnmark Platform (Fig. 9), data from Ørn Formation dolostone samples partially overlap with the field for contemporaneous seawater, but also form a highly linear array that partly overlaps with analyzed poikilotopic calcite cement. These dolostone and colinear calcite data are collectively interpreted to represent a mixing line between pure dolostone and pure calcite cement from microdrilling. The end-member pure poikilotopic calcite cement forms a vertical line in C–O isotope space interpreted to represent the combined effect of meteoric diagenesis and incorporation of varying amounts of carbon sourced from organic matter oxidation, potentially related to hydrocarbon charging. These $\delta^{13}C$ data from the poikilotopic calcite marginally overlap with those reported by Hodgskiss et al. (2022) for calcite spar associated with native sulfur in IKU drill core samples, which largely cluster between −10 and −20‰. Although both populations of calcite ultimately incorporated oxidized organic carbon, poikilotopic calcite samples from the seafloor sample set form a distinctly vertical array, whereas calcite spar samples from the IKU cores form a cluster of more $\delta^{13}C$ negative data.

5.4. Integrating geochronologic, isotopic, paragenetic and tectonic records in the Barents Sea

Each of the previously discussed proxies and techniques ($\delta^{13}C$, $\delta^{18}O$, detailed petrography, U–Pb carbonate dating, and burial history modelling) are very useful for understanding the paragenetic history and tectonic record of the Loppa High and Finnmark Platform, but ultimately each can only inform on limited aspects of this history. Combining these methods allows for a much more complete reconstruction of the post-depositional history of these sedimentary rocks by constraining both the relative and absolute timing of diagenetic events, and directly linking them to ancient geochemical and tectonic processes occurring in the Barents Sea region.

One of the largest and most important tectonic events to occur on the Loppa High was uplift around the P-T boundary that resulted in significant erosion of the Ørn and Falk formations and redeposition as the P-T breccio-conglomerate. Two measured ages of ca. 240 Ma for calcite cement filling intraclast spaces within this unit confirm the timing of this significant uplift event and indicate that precipitation of the poikilotopic and sparry calcite occurred during the early phase of burial that followed this event (Fig. 10). A relatively shallow burial depth during precipitation of these calcite cements is also consistent with the recorded C–O isotope systematics, which suggest influence by meteoric waters from the surface. One dolomicrite clast from the P-T breccio-conglomerate provided an age of 254 Ma (albeit with large errors of ± 56 Ma), possibly representing a diagenetic event that occurred during uplift, reworking on the surface, or shallow burial, although we note that the uncertainties are large enough to include deposition of the Ørn Formation. After formation of calcite cements in the P-T breccio-conglomerate, it appears that almost 200 million years passed without the formation of carbonate cements, surprising given that this time interval includes a phase of progressive burial and rapid uplift. Although it is possible that carbonate cements formed during this time and were not dated (e.g., due to low U concentrations), no other significant carbonate cement forming episodes were identified during petrographic study. In any case, the next major episode of cement formation occurred ca. 75 to 45 Ma (Fig. 10), when calcite cement formed in the Ørn Formation. Based on the modelled burial history, this broadly corresponds to an episode of burial and subsequent uplift during the Paleogene; this link is further supported by C–O isotope systematics that are markedly different from calcite cements of the P-T breccio-conglomerate, and show strong covariation between C and O. This is supported by markedly different C–O isotope systematics, with the Ørn Formation calcite recording precipitation of calcite cement under increasing burial depths/temperatures during the Cretaceous and Paleogene.

Samples from the seafloor of the Finnmark Platform record an approximately 200-million-year gap between deposition and dolomitization of the Ørn Formation ca. 304-296 Ma, and the formation of calcite cements ca. 100 Ma (Fig. 11). Ascribing this generation of cement to a particular event is difficult, as there is no significant change in the modelled burial depth ca. 100 Ma. The vertical C–O isotope array is consistent with meteoric diagenesis, but these sediments are predicted to have been buried to a depth of >1000 m. One possibility, albeit highly speculative, is that increased fluid flow activity associated with the emplacement of the High Arctic Large Igneous Province resulted in fluid flow and precipitation of this poikilotopic calcite cement. This is broadly supported by K–Ar ages from magmatic units in Svalbard and Franz Josef Land that range from 140 to 90 Ma (Maher and Harmon, 2001; Senger and Galland, 2022, and references therein). Alternatively, the modelled burial history may be incomplete and not capture the full record of events for the Finnmark Platform. A final possibility is that this is related to hydrocarbon 'charging' in the Finnmark Platform (Henriksen et al., 2024), and this C–O isotope array resulted from the precipitation of calcite cement with varying proportions of C sourced from oxidation of hydrocarbons. In any case, this event is clearly distinct from the formation of calcite spar in the IKU cores, as it is not associated with anhydrite nor native sulfur, is approximately 50 Myr older, and records a distinct C–O isotope trend.

5.5. Exploring locally incomplete records of diagenesis

When comparing different sample sets from within the same region (Table 1 and Figs. 10 and 11), strikingly different cement ages are recorded. For example, poikilotopic calcite of the Ørn Formation from the seafloor of the Finnmark platform record cement ages of 100 Ma, while calcite spar from the same formation in drill core <10 km away record ages between ca. 55 to 15 Ma. In contrast, the three ages obtained from calcite cements in the Ørn Formation on the Loppa High from two different drill cores overlap within 2σ uncertainties, and calcite cements within the P-T breccio-conglomerate from two different drill cores also overlap within 2σ uncertainties.

We interpret these different ages to represent the local occlusion of fluid pathways during the precipitation of cements, resulting in redirection of fluids along different pathways. If correct, this would suggest that while the overall mechanisms driving the precipitation or reprecipitation of carbonate minerals are occurring on a regional scale, their manifestation is sometimes only local in scale and can change over distances of <10 km, despite being on the same structural element and

presumably experiencing near-identical burial histories. This may be particularly true for the case of hydrocarbon-derived calcite spar in the IKU cores, which required abundant dissolved sulfate that was locally sourced through dissolution of anhydrite. More broadly, this suggests that the collection of samples from a single location/drill core can be insufficient for studies aiming to understand the diagenetic history of sedimentary carbonate rocks.

6. Conclusion

The data presented here refine the understanding of diagenetic carbonate mineral formation on the Loppa High and Finnmark Platform, both temporally and mechanistically. The Loppa High is marked by precipitation of poikilotopic calcite ca. 250 Ma that formed during early burial after P-T uplift, and a second generation of poikilotopic calcite that formed ca. 70–40 Ma and corresponds to a much later burial event in the latest Cretaceous to Paleogene. On the Finnmark Platform, samples collected from the seafloor record significantly different records than studied IKU drill cores ~10 km away. Whereas seafloor samples of the Ørn Formation record a calcite precipitation event ca. 100 Ma, the IKU core samples only record an event ca. 55 to 15 Ma. Analyses of dolomicrite often yielded large uncertainties and only broadly corresponded to the accepted biostratigraphic ages, indicating that while U–Pb carbonate geochronology can be highly effective for analyses of calcite cements, it is markedly less useful for fine grained, dolomitized sediments that are not matrix-matched to standard reference materials and contain contaminating impurities such as detrital clays.

While the new data presented here refine our understanding of the diagenetic histories of these two regions, they also underscore the complexities of 'piecing together' diagenetic histories in general. Most prominently, the absence of carbonate cements for certain major burial events is surprising, and could correspond to either a biased sample set, or that some burial events simply were not associated with the formation of diagenetic carbonates; both possibilities underline the importance of comprehensive sample sets. Conversely, some carbonate cements are not associated with burial events at all and are instead linked to hydrocarbons, which have their own inherent complexities due to the many distinct mechanisms that can produce strongly negative $\delta^{13}C$ values. In any case, the systematic application of these techniques shows great promise for elucidating diagenetic processes and contextualizing them within the regional geology.

CRediT authorship contribution statement

Malcolm S.W. Hodgskiss: Writing – original draft, Visualization, Methodology, Investigation, Formal analysis, Data curation, Conceptualization. **Nick M.W. Roberts:** Writing – review & editing, Methodology, Formal analysis, Data curation. **Michał Matysik:** Writing – review & editing, Writing – original draft, Investigation, Formal analysis, Data curation. **Päärn Paiste:** Writing – original draft, Methodology, Formal analysis, Data curation, Writing – original draft, Conceptualization. **Niels Rameil:** Writing – original draft, Conceptualization. **Erik Hammer:** Visualization, Formal analysis, Conceptualization. **Jon Halvard Pedersen:** Writing – original draft, Conceptualization. **Harald Brunstad:** Writing – original draft, Project administration, Investigation, Conceptualization.

Declaration of competing interest

The authors declare that they have no known competing financial interests or personal relationships that could have appeared to influence the work reported in this paper.

Data availability

Supplementary data file is included.

Acknowledgements

Atle Mørk is thanked for assistance with sampling of IKU drill core materials.

Appendix A. Supplementary data

Supplementary data to this article can be found online at https://doi.org/10.1016/j.marpetgeo.2024.106892.

References

Bojanowski, M.J., Barczuk, A., Wetzel, A., 2014. Deep-burial alteration of early-diagenetic carbonate concretions formed in Palaeozoic deep-marine greywackes and mudstones (Bardo Unit, Sudetes Mountains, Poland). Sedimentology 61, 1211–1239. https://doi.org/10.1111/sed.12098.

Brunstad, H., Rønnevik, H.C., 2024. Loppa high composite Tectono-sedimentary element, Barents Sea. Geological Society 57 (M57), 2020–2023. https://doi.org/10.1144/M57-2020-3. London, Memoirs.

Bugge, T., Mangerud, G., Elvebakk, G., Mørk, A., Nilsson, I., Fanavoll, S., Vigran, J.O., 1995. The upper Palaeozoic succession on the Finnmark platform, Barents Sea. Nor. Geol. Tidsskr. 75, 3–30.

Buggisch, W., Wang, X., Alekseev, A.S., Joachimski, M.M., 2011. Carboniferous–permian carbon isotope stratigraphy of successions from China (yangtze platform), USA (Kansas) and Russia (moscow basin and urals). Palaeogeogr. Palaeoclimatol. Palaeoecol. 301, 18–38. https://doi.org/10.1016/j.palaeo.2010.12.015.

Cavanagh, A.J., Di Primio, R., Scheck-Wenderoth, M., Horsfield, B., 2006. Severity and timing of cenozoic exhumation in the southwestern Barents Sea. J. Geol. Soc. 163, 761–774. https://doi.org/10.1144/0016-76492005-146.

Clark, S.A., Glørstad-Clark, E., Faleide, J.I., Schmid, D., Hartz, E.H., Fjeldskaar, W., 2014. Southwest Barents Sea rift basin evolution: comparing results from backstripping and time-forward modelling. Basin Res. 26, 550–566.

Cohen, K.M., Finney, S.C., Gibbard, P.L., Fan, J.-X., 2013. The ICS International Chronostratigraphic Chart. updated. ver2023/06. https://stratigraphy.org/. (Accessed 12 October 2023).

Drost, K., Chew, D., Petrus, J.A., Scholze, F., Woodhead, J.D., Schneider, J.W., Harper, D. A.T., 2018. An image mapping approach to U-Pb LA-ICP-MS carbonate dating and applications to direct dating of carbonate sedimentation. G-cubed 19, 4631–4648. https://doi.org/10.1029/2018GC007850.

Ehrenberg, S.N., Pickard, N.A.H., Svånå, T.A., Oxtoby, N.H., 2002. Cement geochemistry of photozoan carbonate strata (upper carboniferous-lower permian), Finnmark carbonate platform, Barents Sea. J. Sediment. Res. 72, 95–115. https://doi.org/10.1306/050701720095.

Elisha, B., Nuriel, P., Kylander-Clark, A., Weinberger, R., 2021. Towards in situ U–Pb dating of dolomite. Geochronology 3, 337–349. https://doi.org/10.5194/gchron-3-337-2021.

Gabrielsen, R.H., Færseth, R.B., Jensen, L.N., Kalheim, J.E., Riis, F., 1990. Structural elements of the Norwegian continental shelf. Part I: the Barents Sea region. Norwegian Pet. Directorate Bull. 6, 33 pp.

Glørstad-Clark, E., Faleide, J.I., Lundschien, B.A., Nystuen, J.P., 2010. Triassic seismic sequence stratigraphy and paleogeography of the western Barents Sea area. Mar. Petrol. Geol. 27, 1448–1475. https://doi.org/10.1016/j.marpetgeo.2010.02.008.

Guillong, M., Wotzlaw, J.-F., Looser, N., Laurent, O., 2020. Evaluating the reliability of U–Pb laser ablation inductively coupled plasma mass spectrometry (LA-ICP-MS) carbonate geochronology: matrix issues and a potential calcite validation reference material. Geochronology 2, 155–167. https://doi.org/10.5194/gchron-2-155-2020.

Henriksen, E., Ktenas, D., Nielsen, J.K., 2024. Finnmark platform composite tectono-sedimentary element, Barents Sea. Geological Society 20. https://doi.org/10.1144/M57-2020-20. London, Memoirs 57, M57-2020.

Henriksen, E., Ryseth, A.E., Larssen, G.B., Heide, T., Rønning, K., Sollid, K., Stoupakova, A.V., 2011. Chapter 10 Tectonostratigraphy of the greater Barents Sea: implications for petroleum systems. Geological Society, London, Memoirs 35, 163–195. https://doi.org/10.1144/M35.10.

Hill, C.A., Polyak, V.J., Asmerom, Y., Provencio, P., 2016. Constraints on a Late Cretaceous uplift, denudation, and incision of the Grand Canyon region, southwestern Colorado Plateau, USA, from U-Pb dating of lacustrine limestone. Tectonics 35, 896–906. https://doi.org/10.1002/2016TC004166.

Hodgskiss, M.S., Roberts, N.M., Paiste, P., Rameil, N., Hammer, E., Brunstad, H., Lepland, A., 2024. Direct dating of deposition and rift-related alteration of fossil-barren red bed units in the North Sea. J. Geol. Soc. 181 (1), jgs2023–052.

Hodgskiss, M.S.W., Thiagarajan, N., Wang, Y., Rameil, N., Brunstad, H., Hammer, E., Pedersen, J.H., Kirsimae, K., Mørk, A., Lepland, A., 2022. Time constraints on hydrocarbon migration and caprock formation recorded by calcite spar in a Carboniferous–Permian carbonate-evaporite succession, Finnmark Platform, Barents Sea. Geology 50 (1), 1234–1238. https://doi.org/10.1130/G50244.

Hollis, C., 2011. Diagenetic controls on reservoir properties of carbonate successions within the Albian–Turonian of the Arabian Plate. Petrol. Geosci. 17 (3), 223–241. https://doi.org/10.1144/1354-079310-032.

Indrevær, K., Gabrielsen, R.H., Faleide, J.I., 2017. Early Cretaceous synrift uplift and tectonic inversion in the Loppa High area, southwestern Barents Sea, Norwegian shelf. J. Geol. Soc. 174, 242–254. https://doi.org/10.1144/jgs2016-066.

Ktenas, D., Nielsen, J.K., Henriksen, E., Meisingset, I., Schenk, O., 2023. The effects of uplift and erosion on the petroleum systems in the southwestern Barents Sea: insights from seismic data and 2D petroleum systems modelling. Mar. Petrol. Geol. https://doi.org/10.1016/j.marpetgeo.2023.106535 (in press).

Lammers, S., Suess, E., Hovland, M., 1995. A large methane plume east of Bear Island (Barents Sea): implications for the marine methane cycle. Geol. Rundsch. 84, 59–66. https://doi.org/10.1007/BF00192242.

Lan, Z., Wu, S., Roberts, N.M., Zhang, S., Cao, R., Wang, H., Yang, Y., 2022. Geochronological and geochemical constraints on the origin of highly 13Ccarb-depleted calcite in basal Ediacaran cap carbonate. Geol. Mag. 159 (8), 1323–1334.

Lan, Z., Wu, S., Wang, F., Liu, B., Shi, K., Sun, J., Cao, R., Li, X.H., 2023. A ca. 290 Ma hydrothermal calcite in Cambrian dolostone. Mar. Petrol. Geol. 147, 106011.

Larssen, G.B., Elvebakk, G., Henriksen, L.B., Kristensen, S.-E., Nilsson, I., Samuelsberg, T. J., Svånå, T.A., Stemmerik, L., Worsely, D., 2002. Upper Palaeozoic lithostratigraphy of the Southern part of the Norwegian Barents Sea 3–43 s.

Larssen, G.B., Elvebakk, G., Henriksen, L.B., Kristensen, S., Nilsson, I., Samuelsberg, T.J., Svåna, T.A., Stemmerik, L., Worsley, D, 2005. Upper Palaeozoic lithostratigraphy of the Southern part of the Norwegian Barents Sea. Geol. Surv. Norway Bull. 444.

Lasabuda, A.P.E., Johansen, N.S., Laberg, J.S., Faleide, J.I., Senger, K., Rydningen, T.A., Patton, H., Knutsen, S.-M., Hanssen, A., 2021. Cenozoic uplift and erosion of the Norwegian Barents Shelf – a review. Earth Sci. Rev. 217, 103609 https://doi.org/10.1016/j.earscirev.2021.103609.

Lippard, S.J., Prestvik, T., 1997. Carboniferous dolerite dykes on Magerøy: new age determination and tectonic significance. Nor. Geol. Tidsskr. 77, 159–163.

Liu, J., Li, Z., Cheng, L., Li, J., 2017. Multiphase calcite cementation and fluids evolution of a deeply buried carbonate reservoir in the upper ordovician lianglitag formation, tahe oilfield, tarim basin, NW China. Geofluids 2017, e4813235. https://doi.org/10.1155/2017/4813235.

Lohmann, K.C., 1988. Geochemical patterns of meteoric diagenetic systems and their application to studies of paleokarst. In: James, N.P., Choquette, P.W. (Eds.), Paleokarst. Springer, New York, NY, pp. 58–80. https://doi.org/10.1007/978-1-4612-3748-8_3.

Lopes, G., McLean, D., Mangerud, G., Clayton, G., 2018. A new Mississippian biozonal scheme for the Finnmark Platform, Norway – palynostratigraphic integration of exploration wells 7128/4-1 and 7128/6-1. Mar. Petrol. Geol. 92, 94–108. https://doi.org/10.1016/j.marpetgeo.2018.02.004.

Lucia, F.J., Kerans, C., Jennings Jr, J.W., 2003. Carbonate reservoir characterization. Journal of petroleum technology 55 (6), 70–72. https://doi.org/10.2118/82071-JPT.

Maher, Jr., Harmon, D., 2001. Manifestations of the Cretaceous high arctic large igneous Province in svalbard. J. Geol. 109, 91–104. https://doi.org/10.1086/317960.

Matysik, M., Stemmerik, L., Olaussen, S., Rameil, N., Gianotten, I.P., Brunstad, H., 2021. Cherts, spiculites, and collapse breccias – porosity generation in upper Permian reservoir rocks, Gohta discovery, Loppa High, south-western Barents Sea. Mar. Petrol. Geol. 128, 105043 https://doi.org/10.1016/j.marpetgeo.2021.105043.

Midtkandal, I., Faleide, J.I., Faleide, T.S., Serck, C.S., Planke, S., Corseri, R., Dimitriou, M., Nystuen, J.P., 2019. Lower Cretaceous Barents Sea strata: epicontinental basin configuration, timing, correlation and depositional dynamics. Geol. Mag. 157, 458–476. https://doi.org/10.1017/S0016756819000918.

Müller, R., Klausen, T.G., Faleide, J.I., Olaussen, S., Eide, C.H., Suslova, A., 2019. Linking regional unconformities in the Barents Sea to compression-induced forebulge uplift at the Triassic-Jurassic transition. Tectonophysics 765, 35–51. https://doi.org/10.1016/j.tecto.2019.04.006.

Pan, L., Hu, A., Liang, F., Jiang, L., Hao, Y., Feng, Y., Shen, A., Zhao, J., 2021. Diagenetic conditions and geodynamic setting of the middle Permian hydrothermal dolomites from southwest Sichuan Basin, SW China: insights from in situ U–Pb carbonate geochronology and isotope geochemistry. Mar. Petrol. Geol. 129, 105080 https://doi.org/10.1016/j.marpetgeo.2021.105080.

Pan, L., Shen, A., Zhao, J.X., Hu, A., Hao, Y., Liang, F., Feng, Y., Wang, X., Jiang, L., 2020. LA-ICP-MS U-Pb geochronology and clumped isotope constraints on the formation and evolution of an ancient dolomite reservoir: the Middle Permian of northwest Sichuan Basin (SW China). Sediment. Geol. 407, 105728 https://doi.org/10.1016/j.sedgeo.2020.105728.

Paton, C., Hellstrom, J., Paul, B., Woodhead, J., Hergt, J., 2011. Iolite: Freeware for the visualisation and processing of mass spectrometric data. J. Anal. Atom. Spectrom. 26 (12), 2508–2518. https://doi.org/10.1039/C1JA10172B.

Petrus, J.A., Chew, D.M., Leybourne, M.I., Kamber, B.S., 2017. A new approach to laser-ablation inductively-coupled-plasma mass-spectrometry (LA-ICP-MS) using the flexible map interrogation tool 'Monocle. Chem. Geol. 463, 76–93. https://doi.org/10.1016/j.chemgeo.2017.04.02.

Pinedo-González, P., West, A.J., Tovar-Sanchez, A., Duarte, C.M., Sañudo-Wilhelmy, S. A., 2018. Concentration and isotopic composition of dissolved Pb in surface waters of the modern global ocean. Geochem. Cosmochim. Acta 235, 41–54. https://doi.org/10.1016/j.gca.2018.05.005.

Roberts, N.M.W., Drost, K., Horstwood, M.S.A., Condon, D.J., Chew, D., Drake, H., Milodowski, A.E., McLean, N.M., Smye, A.J., Walker, R.J., Haslam, R., Hodson, K., Imber, J., Beaudoin, N., Lee, J.K., 2020. Laser ablation inductively coupled plasma mass spectrometry (LA-ICP-MS) U–Pb carbonate geochronology: strategies, progress, and limitations. Geochronology 2, 33–61. https://doi.org/10.5194/gchron-2-33-2020.

Roberts, N.M., Rasbury, E.T., Parrish, R.R., Smith, C.J., Horstwood, M.S., Condon, D.J., 2017. A calcite reference material for LA-ICP-MS U-Pb geochronology. Geochem. Geophys. Geosyst. 18 (7), 2807–2814. https://doi.org/10.1002/2016GC006784.

Rochelle-Bates, N., Roberts, N.M.W., Sharp, I., Freitag, U., Verwer, K., Halton, A., Fiordalisi, E., van Dongen, B.E., Swart, R., Ferreira, C.H., Dixon, R., 2021. Geochronology of volcanically associated hydrocarbon charge in the pre-salt carbonates of the Namibe Basin, Angola. Geology 49 (3), 335–340. https://doi.org/10.1130/G48019.1.

Rochelle-Bates, N., Wood, R., Schröder, S., Roberts, N.M., 2022. In situ U–Pb geochronology of Pre-Salt carbonates reveals links between diagenesis and regional tectonics. Terra. Nova 34 (4), 271–277. https://doi.org/10.1111/ter.12586.

Rønnevik, H., Jacobsen, H.-P., 1984. Structural highs and basins in the western Barents Sea. In: Spencer, A.M. (Ed.), Petroleum Geology of the North European Margin. Springer, Netherlands, Dordrecht, pp. 19–32. https://doi.org/10.1007/978-94-009-5626-1_3.

Sayago, J., Di Lucia, M., Mutti, M., Cotti, A., Sitta, A., Broberg, K., Przybylo, A., Buonaguro, R., Zimina, O., 2012. Characterization of a deeply buried paleokarst terrain in the Loppa High using core data and multiattribute seismic facies classification. AAPG (Am. Assoc. Pet. Geol.) Bull. 96, 1843–1866. https://doi.org/10.1306/02271211137.

Senger, K., Galland, O., 2022. Stratigraphic and spatial extent of HALIP magmatism in central spitsbergen. G-cubed 23, e2021GC010300. https://doi.org/10.1029/2021GC010300.

Stemmerik, L., Vigran, J.O., Piasecki, S., 1991. Dating of late paleozoic rifting events in the North Atlantic: new biostratigraphic data from the uppermost devonian and carboniferous of east Greenland. Geology 19, 218–221. https://doi.org/10.1130/0091-7613(1991)019<0218:DOLPRE>2.3.CO;2.

Stemmerik, L., Worsley, D., 1989. Late palaeozoic sequence correlations, North Greenland, svalbard and the Barents shelf. In: Collinson, J.D. (Ed.), Correlation in Hydrocarbon Exploration. Springer, Netherlands, Dordrecht, pp. 99–111. https://doi.org/10.1007/978-94-009-1149-9_10.

Su, A., Chen, H., Feng, Y.X., Zhao, J.X., Wang, Z., Hu, M., Jiang, H., Nguyen, A.D., 2022. In situ U-Pb dating and geochemical characterization of multi-stage dolomite cementation in the Ediacaran Dengying Formation, Central Sichuan Basin, China: constraints on diagenetic, hydrothermal and paleo-oil filling events. Precambrian Res. 368, 106481 https://doi.org/10.1016/j.precamres.2021.106481.

Su, A., Chen, H., Feng, Y.X., Zhao, J.X., Nguyen, A.D., Wang, Z., Long, X., 2020. Dating and characterizing primary gas accumulation in Precambrian dolomite reservoirs, Central Sichuan Basin, China: insights from pyrobitumen Re-Os and dolomite U-Pb geochronology. Precambrian Res. 350, 105897 https://doi.org/10.1016/j.precamres.2020.105897.

Xiong, S.F., Jiang, S.Y., Zhao, J.X., Niu, P.P., Ma, Y., Bai, X.Y., 2023. Dating Precambrian sedimentary carbonate strata by in situ U–Pb isotopes of dolomite. Precambrian Res. 393, 107088 https://doi.org/10.1016/j.precamres.2023.107088.

Zhang, J., Wang, J., Zheng, B., Sheng, Q., Wei, H., Shen, L., Xiong, S., Mansour, A., 2023. Age assignment of dolomite in palaeo-reservoirsof the Qiangtang Basin: new evidence from palaeontology and carbonate in situ U-Pb dating. Mar. Petrol. Geol. 158, 106545 https://doi.org/10.1016/j.marpetgeo.2023.106545.